Effects of KOH etching on the properties of Ga-polar n-GaN surfaces

Grigore Moldovan, Martin Roe, Ian Harrison, Menno Kappers, Colin John Humphreys, P D Brown

Effects of KOH etching on the properties of Ga-polar n-GaN surfaces

Journal:	*Philosophical Magazine & Philosophical Magazine Letters*
Manuscript ID:	TPHM-05-Sep-0402.R2
Journal Selection:	Philosophical Magazine
Date Submitted by the Author:	06-Dec-2005
Complete List of Authors:	Moldovan, Grigore; University of Cambridge, Department of Materials Science and Metallurgy; University of Nottingham, School of Mechanical, Materials, Manufacturing Engineering and Management Roe, Martin; University of Nottingham, School of Mechanical, Materials and Manufacturing Engineering Harrison, Ian; University of Nottingham, School of Mechanical, Materials and Manufacturing Engineering Kappers, Menno; University of Cambridge, Department of Materials Science and Metallurgy Humphreys, Colin; University of Cambridge, Department of Materials Science and Metallurgy Brown, P; University of Nottingham, School of Mechanical, Materials, Manufacturing Engineering and Management
Keywords:	surface properties, contact mechanics, electrical properties, GaN, metallization
Keywords (user supplied):	KOH surface treatment, non-radiative recombination

Effects of KOH etching on the properties of Ga-polar n-GaN surfaces

G. MOLDOVAN[1,2], M. J. ROE[1], I. HARRISON[1], M. KAPPERS[2], C. J HUMPHREYS[2] and P. D. BROWN[1]

[1] School of Mechanical, Materials and Manufacturing Engineering, University of Nottingham, University Park, Nottingham, NG7 2RD, UK

[2] Department of Materials Science and Metallurgy, University of Cambridge, Pembroke Street, Cambridge, CB2 3QZ, UK

The effects of a KOH treatment on the properties of n-type GaN surfaces and associated Au/n-GaN contacts have been investigated by means of X-ray photoelectron spectroscopy, atomic force microscopy, reflection high-energy-electron diffraction, current-voltage and electron-beam-induced current characterisation. Ga-polar surfaces grown by molecular beam epitaxy and metal-organic chemical vapour deposition were compared. A decrease in electron barrier height and an increase in non-radiative recombination properties of Au/n-GaN contacts were found with KOH treatment, correlated with an increase of surface Ga vacancies, an increase of surface N-H_2 content and a decrease of surface C contamination. A 0.3 eV shift in the Ga3d peak position towards the valence band and a reduction in the dislocation contrast were observed for the case of molecular-beam-epitaxy-grown GaN only, demonstrating that surface Ga vacancies and threading dislocations play only a limited role in defining the resultant metal/GaN contact properties. Accordingly, the surface atomic content and the resulting surface states following KOH treatment should be taken into consideration when appraising the electrical properties of n-GaN surfaces and the performance of associated metallic contacts.

1. Introduction

The performance of GaN-based devices is significantly influenced by the quality of the metallic contacts used to make connection to power sources and/or other devices [1]. The electrical properties of metal/n-GaN contacts depend on a wide variety of processing parameters, such as cleaning and etching of the GaN surface [2, 3], the composition and thickness of the metallic contacting layers, and the annealing temperature and atmosphere used to activate the contact. Because enhanced diffusion couple metallization layers and annealing conditions have been identified to gain improved contact performance, increased attention is also being given to the preparation of GaN surfaces prior to metallization. For example, previous work has shown that ohmic contacts of lower resistance can be obtained by making contact to plasma or wet-etched surfaces [4].

Detailed investigations are required to appraise the intimate relationship between the chemical treatment employed, the resulting chemical/structural modifications to the GaN surface and the electrical properties of the contacts. Whilst detailed understanding has been gained on the effects of surface cleaning, for example HCl [5] or HF [6] treatments, much less is known about the consequences of surface etching, for example KOH or plasma treatments, partly because of the dual action of the removal of GaN material combined with surface cleaning. One approach to address this problem is to compare cleaned and etched surfaces in order to assess the consequences of the removal of GaN material on contact performance. Furthermore, in order to appraise the effects of GaN surface treatment on the performance of electrical contacts, it is helpful to use metallic contacts that do not alloy with GaN, such as Au [7] or Pt [8], thus avoiding further modification to the GaN material.

The present work studies the mechanisms that determine the barrier height by investigating the effects of KOH etching on the properties of n-GaN surfaces and associated Au/n-GaN Schottky contacts. To investigate the role of KOH etching beyond surface cleaning, the KOH treatment was used in conjunction with an HCl clean (samples denoted as 'KOH treated') and compared with a reference HCl clean (samples denoted as 'reference'). Hence, reference and KOH-treated n-GaN surfaces have been investigated, initially with regard to sample surface composition, bonding states, morphology and crystalline structure. Consideration has then given to the electrical properties of Au Schottky contacts deposited onto these treated n-GaN surfaces, in order to appraise the respective electron barrier heights and the extent of non-radiative recombination activity. In this context, surfaces of Ga-polar GaN/sapphire grown by molecular beam epitaxy (MBE) and metal-organic chemical vapour deposition (MOCVD) are also compared.

2. Experimental

The starting MBE GaN/sapphire wafer was 2.5 µm thick and exhibited an n-type carrier concentration of 6.4 x 10^{16} cm.$^{-3}$ The MOCVD GaN/sapphire (0001) wafer was 3 µm thick with a 0.9 µm thick Si-doped capping layer and an estimated n-type carrier concentration of 1 x 10^{17} cm.$^{-3}$ Cleaved samples were first sequentially degreased using a standard procedure of ultrasonic baths of lotoxane, methanol, acetone, propanol and de-ionized water, for three minutes each. The subsequent KOH treatment consisted of sample dipping in a 4 molar solution of KOH and de-ionized water for 1 minute at 60ºC, followed by a 1 minute dip in de-ionized water, then blowing dry using N_2. The cleaning process consisted of dipping into a 37 % solution of HCl and de-ionised water for three minutes, again blowing dry using N_2. The surface chemistry of the etched GaN samples was appraised by X-ray photoelectron spectroscopy (XPS) using a VG scientific ESCALAB spectrometer using AlKα X-rays at an anode voltage of 10 kV and a filament emission current of 20 mA. Samples were loaded into the XPS chamber immediately after the final HCl cleaning stage. Surface morphology was investigated by atomic force microscopy (AFM) using a Dimension AFM in tapping mode. The near-surface crystallographic structure of samples was assessed by means of reflection high-energy-electron diffraction (RHEED), performed within a modified Jeol 2000fx transmission electron microscope (TEM), using the glancing-angle diffraction of electrons at the surface of specimens mounted vertically just below the projector lens.

For the purpose of complementary current-voltage (*I-V*) measurements and electron-beam-induced current (EBIC) investigations, the sample set was replicated using adjacent areas from the

same wafers. Glass shadow masks were used to define Au Schottky contacts, along with Ti ohmic pads for ground connection. Au was deposited simultaneously on all samples at a rate of 3 nm/s, to a thickness of 125 nm, using a thermal evaporator at a chamber pressure of 4 x 10^{-6} Torr. Ti was deposited at 0.7 nm/s, to a thickness of 200 nm, using an e-beam evaporator at a chamber pressure of 2.5 x 10^{-6} Torr. EBIC measurements were performed using a Jeol 6400 scanning electron microscope (SEM) operating at an acceleration voltage of 10 kV and a Matelect IV5 low-noise current amplifier.

3. Results

3.1. Characterization of n-GaN surfaces

The acquired XPS survey spectra covering the 0-1100 eV binding energy range were dominated by N and Ga peaks, with significant levels of C and traces of O and Cl, in all cases. The atomic weight percentages (atom wt %) of the surface species were determined using peak areas and sensitivity factors appropriate for N1s, Ga3d, C1s, O1s and Cl2p photoelectron lines, as summarized in Table 1. These elemental ratios are comparative and do not represent absolute stoichiometry since the photoionization cross-section and transmission function of the spectrometer for each element are not taken into account. However, a distinct trend is revealed, with the KOH treatment resulting in an increase of the N surface content and a decrease of the Ga surface content for the case of both MBE and MOCVD samples, in agreement with [9] for the case of MOCVD-grown GaN. It is also evident, following KOH treatment, that the surface C content decreased slightly for the case of the MBE-grown GaN and significantly for the case of the MOCVD-grown sample. Variations in the O and Cl surface content were also detected, but these values were below 1 %, and on the scale of the sensitivity of this XPS experimental arrangement. No remnant K content was detected as a consequence of the KOH treatment.

'[Insert table 1 about here]'

Detailed XPS scans of the O1s, Ga3d and N1s peaks were recorded, with reference to the C1s peak at 285 eV, to appraise the bonding state of the surface atoms (Figures 1a-f). The N1s peaks were de-convoluted into four contributions in all cases: i.e. an N-H_2 ionization peak, an N-Ga ionization peak and two Auger Ga peaks (Figures 1a,d). No change in the binding energies of these peaks was observed as a function of GaN growth process or surface treatment, although a significant increase in the N-H_2/N-Ga ratio of ~0.1 was detected as a consequence of the KOH treatment, from 0.66 to 0.75 for the case of MBE-grown GaN and from 0.48 to 0.59 for the case of MOCVD-grown GaN, in agreement with [10]. The Ga3d peaks were similarly de-convoluted into the contributions of metallic Ga, GaN and Ga_2O_3 (Figures 1b,e). For the MBE-grown GaN sample after KOH treatment, in particular, the Ga3d binding energy showed a shift of -0.3eV. A corresponding binding energy shift for the KOH-treated MOCVD grown GaN was not observed for the processing conditions applied in this work, but shifts of -0.3 eV and -0.4 eV have been reported for MOCVD-grown GaN following more aggressive treatment in KOH [9-11]. The binding energy of the O1s peak remained unchanged with sample growth process or surface treatment (Figures 1c,f). For the case of the reference MBE-grown sample only, the O1s peak could be de-convoluted into three contributions: i.e. a chemisorbed O peak at 530.1 eV, a Ga_2O_3 peak at 531.9 eV and an OH peak at 533.1 eV, respectively. The KOH etching treatment was found to eliminate the O and OH peaks, although the overall O content of the MBE-grown surface remained constant, as determined from survey spectra, which is again consistent with [10].

'[Insert figure 1 about here]'

Figures 2a,b present 1 x 1 µm AFM height-amplitude images of reference HCl-cleaned MBE and MOCVD GaN samples. The surface morphology of the MBE-grown sample (Fig. 2a) is markedly rougher than the MOCVD sample (Fig 2b), with rms values of 15.0 nm and 0.62 nm, respectively. The morphology of Figure 2a is indicative of the fine-scale cellular grain structure of such MBE-grown GaN/sapphire samples, whilst MOCVD-grown GaN/sapphire samples generally exhibit a much larger grained crystalline structure with a significantly lower threading dislocation content. Accordingly, Figure 2b shows a much smoother step flow surface with terraces occasionally observed to terminate at features considered to be threading dislocations containing a screw component [12]. The KOH treatment was found to modify the MBE surface slightly. Figure 3 shows a 1 x 1 µm AFM height-

amplitude image of the KOH etched MBE sample, revealing the development of flat-bottomed hexagonal pits, of ~3.5 x 10^9 cm^{-2} density and ~40 nm average depth in this instance. The sample rms roughness was reduced by 1.8 nm. Conversely, the KOH treatment was found not to change the morphology of the MOCVD surface within the detection limits of AFM.

'[Insert figures 2 and 3 about here]'

The near surface crystal structures of the reference and KOH-treated samples were appraised using RHEED. Figures 4a.b show $<1\bar{1}20>$ GaN zone-axis diffraction patterns acquired for the reference MBE and MOCVD samples, respectively. The MBE-grown sample exhibited a well-defined spot pattern indicative of single-crystal hexagonal material with a rough surface (Fig 4a) in keeping with the AFM measurements, whilst the MOCVD-grown sample exhibited a streaky, diffuse spot pattern with a strong kikuchi band background, consistent with single-crystal hexagonal material with a very smooth surface (Fig 4b). It is noted, however, that streaks perpendicular to a growth surface are more precisely attributable to material that is not perfectly flat, but with slight local miss-orientation combined with some degree of surface disorder [13]. There were no observable differences between the RHEED patterns acquired from the reference and KOH-treated GaN surfaces, indicating that the near-surface crystallographic structures of these MBE- and MOCVD-grown samples, respectively, were not changed by the applied surface treatments.

'[Insert figure 4 about here]'

3.2. Characterization of Au/n-GaN contacts

To appraise the consequences of KOH etching on the resultant electrical activity of metal/n-GaN contacts, the surface treatment of this GaN sample set was replicated under identical conditions, using material from the same wafers, prior to the deposition of Au and Ti pads to form suitable rectifying and ohmic contacts, respectively. The *I-V* responses of the contacted samples were recorded at room temperature under ambient illumination (Figure 5). The recorded curves demonstrate larger leakage currents for the Au contacted MBE GaN samples than the corresponding MOCVD samples (i.e. Au contacts to MOCVD GaN are more strongly rectifying than Au contacts to MBE GaN). Further, the reference samples exhibited smaller leakage currents as compared with the KOH-treated samples for both growth processes (i.e. the KOH treatment results in the formation of more weakly rectifying Au/n-GaN contacts). The associated electron barrier heights were calculated from the [-0.4 V-0.1 V] reverse bias of the *I-V* characteristics, according to the Schottky diode relation

$$J = A^{xx}T^2\exp\left(-\frac{\phi_b}{kT}\right)\exp\left(\frac{eV}{nkT}\right)\left[1-\exp\left(-\frac{eV}{kT}\right)\right]$$

where J is the current density, A^{xx} is the effective Richardson constant (26.4 A/cm^2K^2 for n-GaN), T is the absolute temperature, ϕ_b is the barrier height, k is Boltzmann's constant, n is an ideality factor, e is the electronic charge and V is the applied voltage [14]. Since strong deviations from ideal Schottky behaviour occur under reverse bias, it is considered that the electron barrier heights extracted with this method should only be taken as indicative of trends and not understood as absolute values. Au contacts to MBE-grown n-GaN exhibited barrier heights of 0.75 V and 0.71 V for reference and KOH treated samples, respectively, whilst corresponding Au contacts to MOCVD grown n-GaN showed barrier heights of 0.92 V and 0.74 V for reference and KOH-treated samples, respectively. Thus, smaller electron barriers heights are associated with Au-contacted MBE GaN as compared with MOCVD reference samples, whilst there is a reduction in the electron barrier height after KOH treatment, regardless of growth method.

'[Insert figure 5 about here]'

The Au-contacted samples were further investigated by SEM using secondary electron (SE) and EBIC modes of operation. Topographic contrast images obtained in the SE mode (Figs. 6a,b) suggested rough and smooth surfaces for the MBE- and MOCVD-grown GaN samples, respectively, again consistent with the AFM images. EBIC measurements appraising the electrical activity of these samples were performed at a comparatively low accelerating voltage of 10 kV in an attempt to accentuate the contribution of the contacted GaN surface to the EBIC signal. EBIC images taken from

the same areas as SE images revealed a high density of small sub-grains of ~350 nm size for the MBE-grown GaN sample (Fig. 6c) and larger sub-grains of ~1 µm size for the MOCVD grown GaN sample (Figure 6d), again consistent with the differing microstructures of these MBE- and MOCVD-grown GaN/sapphire heterostructures. For the case of the MBE-grown GaN sample, the locations of low EBIC signal appeared to correlate with the position of grain boundaries within the associated SE images [4]. Within the resolution limits of the EBIC experiment, however, the generated images of the non-radiative recombination activity provided no additional features attributable to the effects of the KOH treatment.

'[Insert figure 6 about here]'

EBIC line-scans (Figure 7) were therefore recorded under identical conditions of electron beam current and spot size to quantify the non-radiative recombination at dislocation and dislocation-free sites within each sample. Averaged EBIC signal magnitudes and values for the dislocation contrast, calculated using $C_{\text{dislocation}} = (I_{\text{dislocation-free}} - I_{\text{dislocation}}) / I_{\text{dislocation-free}}$, are summarized in Table 2. The MBE samples exhibited lower values of absolute EBIC current, consistent with a greater level of non-radiative recombination for both dislocation-free and dislocation sites, as compared with the MOCVD samples. In particular, the KOH treatment was associated with an overall reduction in the magnitude of the induced current and a corresponding increase in the non-radiative recombination activity in both cases. Further, a drastic reduction in the contrast associated with dislocations occurred for the case of MBE-grown samples, whilst the contrast associated with dislocations within the MOCVD grown samples appeared independent of the KOH treatment.

'[Insert figure 7 and table 2 about here]'

4. Discussion

The combined AFM, SE and RHEED investigations provide a clear description of the sample surface morphology and near-surface microstructure, whilst *I-V* and EBIC characterization provide evidence for changes in the contact electronic barrier height and the level of non-radiative recombination as a consequence of KOH treatment. Furthermore, XPS data provide clues to changes in the surface chemistry and by implication surface electronic structure, following etching, to help reconcile these observations.

Au contacts to MBE-grown n-GaN exhibited lower electron barrier heights as compared with Au-contacted MOCVD-grown n-GaN, which cannot be explained within the thermionic-emission model for contact operation alone, since the barrier height should not depend on the doping levels of the MBE and MOCVD samples examined here [15]. It is evident that the addition of a KOH treatment to the standard contacting procedure has acted to introduce significant changes in the electrical properties of the Au/n-GaN contacts, acting to lower the barrier height, increase the leakage current and render the contacts less rectifying. Thus, surface chemistry, roughness and defect microstructure, i.e. threading dislocation content, are all initially implicated as parameters affecting the contact properties. In particular, the -0.3 eV shift in the Fermi level of the KOH etched n-GaN MBE surface, as compared with the cleaned surface, demonstrates that the electron barrier height of the resulting contacts is strongly influenced by surface states.

A significant reduction in the Ga surface content was associated with the KOH treatment for both MBE and MOCVD samples, being attributed to the formation and dissolution of a gallium-based hydroxide [10]. This effect was more pronounced for the rougher MBE-grown GaN. A reduction of the surface Ga content also indicates an increase in the number of surface Ga vacancies and an enhancement of a corresponding acceptor level, resulting in the shift of the Fermi level towards the valence band at the free GaN surface. This is consistent with the -0.3eV shift in the Ga3d binding energy identified for the case of MBE-grown GaN following KOH treatment. Furthermore, the *I-V* and EBIC characterisation experiments as applied to Au-contacted n-GaN samples agree with the trend of this XPS data, demonstrating a reduction in electron barrier height and an increase in non-radiative recombination for both MBE- and MOCVD-grown samples following KOH treatment. However, the formation of Ga vacancies might not be the only mechanism of barrier modification, since a reduction in the surface Ga content also correlates with an increase in the surface N content with a corresponding increase in the N-H_2/N-Ga ratio. As also illustrated in Figure 8, there is a distinct

correlation of the increase in the N-H_2/N-Ga ratio following KOH etching with this reduction in the electron barrier height. The key point here is the lack of a Fermi level shift for the case of MOCVD-grown GaN following KOH treatment, alongside a corresponding reduction in the contact barrier height and an increase in the level of non-radiative recombination. This suggests a more pervasive role of N-H_2 centres in defining the contact behaviour in this instance, with this interpretation being sustained by theoretical calculation [16].

'[Insert figure 8 about here]'

The morphology of the rough MBE-grown samples when exposed to KOH treatment was significantly modified with the introduction of flat-bottomed pits, while the overall morphology of the MOCVD-grown surfaces remained largely unaffected, as would be expected for these Ga-polar surfaces of GaN [10]. The position of such pits has previously been associated with the position of mixed threading dislocations [12]. Furthermore, a drastic reduction in the EBIC dislocation contrast was observed for the case of etched MBE-grown GaN (from 12 % to 1 %), whilst the dislocation contrast remained effectively constant (~12 %) for the case of MOCVD-grown GaN following KOH treatment. The indication being that the KOH treatment introduces comparatively more non-radiative recombination centres at dislocation-free regions than at dislocation sites for the MBE etched sample, whilst dislocation and dislocation-free sites within the MOCVD sample are similarly affected under the KOH treatment conditions applied here. As this observation cannot be reconciled in terms of the differing threading dislocation densities within these samples, it is considered that the threading dislocation density does not play a significant role in defining the resultant contact properties. Similarly, this observation cannot be described in terms of amorphous material, since no significant amorphous surface content was detected, before or after the KOH treatment, as indicated by RHEED. Accordingly, surface roughness and surface states are considered to dominate the electronic properties of these contacts.

Even though the chemiabsorbed O and OH surface content of the MBE-grown GaN was effectively removed by the KOH treatment, the overall O content of the MBE-grown surface remained constant, suggesting a stabilized coverage of Ga_2O_3, in agreement with [10]. In this context, it is envisaged that a small amount of atmospheric re-oxidation occurred quickly after the KOH treatment of the MBE sample. Nevertheless, in view of the overall O surface content being less than 1 %, this is not sufficient to be considered as a continuous oxide layer at the Au-GaN interface and hence a model to explain the contact performance based purely on a metal/oxide/semiconductor structure, for example invoking an impurity barrier model, cannot be used in this case.

With regard to the detected surface content of Cl attributed to the cleaning treatment in HCl solution, it has been suggested [5] that Cl halogens tie up Ga dangling bonds at the surface, hindering re-oxidation (as would appear to be the case here). Perhaps of more significance is the C content at the GaN surface. In view of the reduction of the surface C content following the KOH treatment (and corresponding increase in the proportion of N-H_2 surface states) of both MBE- and MOCVD-grown samples, it is suggested that adventitious carbon also has a strong effect on the electrical properties of n-GaN surfaces, and the development of Au/n-GaN contacts.

5. Conclusions

Significant differences in the chemistry of n-GaN surfaces and the electron barrier height and non-radiative recombination properties of Au/n-GaN contacts are identified as a consequence of the addition of a KOH treatment step to the standard GaN cleaning protocol. A decrease in electron barrier height and an increase in non-radiative recombination at the Au/n-GaN contacts occur for both MBE- and MOCVD-grown GaN samples, being partly attributed to an increasingly Ga-poor surface and a corresponding increase in the density of surface acceptors. Whilst this interpretation is sustained by a 0.3 eV shift in the Ga3d peak towards the valence band for the case of MBE-grown GaN, no corresponding shift in the Fermi level was recorded for the Ga3d peak positions for the case of MOCVD-grown GaN in response to the KOH treatment used in this instance. Accordingly, a second contribution to the reduction of the electronic barrier height and the increase in the non-radiative recombination activity is suggested, namely an increase in the N-H_2 surface content and associated decrease in the C content, as a consequence of the KOH treatment for both MBE- and MOCVD-grown

GaN. By comparing KOH-etched and HCl-cleaned surfaces with reference HCl-cleaned surfaces, it has been demonstrated that the KOH treatment has modified the electrical properties of metal/n-GaN contacts and this process cannot be attributed solely to removal of an oxide layer.

Acknowledgements

This work was supported under EPSRC grant GR/M87078 and GR/S25630. We thank J. B. Webb, NRC Ottawa, for the supply of the MBE materials. GM would like to acknowledge R. Broom for most useful discussions on the properties of Schottky contacts and R. Dykeman for depositing the Au layers.

References

[1] S.J. Pearton, F. Ren, A.P. Zhang and K.P. Lee, Mat. Sci. Eng. R30 55-212 (2000)
[2] A.T. Ping, Q Chen, J.W. Yang, M Asif Khan and I Adesida, J. Electron Mat. **27** 4 261-265 (1998)
[3] A.T. Ping, A.C. Schmitz, I. Adesida, M Asif, Q Chen and J.W. Yang, J. Electron Mat. **26** 3 266-271 (1997)
[4] G. Moldovan, I Harrison and P.D. Brown, Inst. Phys. Conf. Ser. 180 577-580 (2003)
[5] S.W. King, J.P. Barnak, M.D. Bremser, K.M. Tracy, C. Ronning, R.F. Davis and R.J. Nemanich, J. Appl. Phys. **84** 9 5248-5260 (1998)
[6] L. Smith, S.W. King, R.J. Nemanich and R.F. Davis, J. Electron. Mat. **25** 5 805-810 (1996)
[7] T.G.G. Maffeis, M.C. Simmonds, S.A. Clark, F. Peiro, P. Haines and P. Parbrook, J. Appl. Phys. **96** 6 3179-3186 (2002)
[8] J. Hilsenbeck, W. Rieger, E. Nebauer, W John, G. Trankle, J. Wurfl, A. Ramakrishan and H Obloh, Phys. Stat. Sol. A 176 183-187 (1999)
[9] K. Rickert, A.B. Ellis, F.J. Himpsel, J. Sun and T.F. Kuech, Appl. Phys. Lett. **80** 2 204-206 (2002)
[10] D. Li, M. Sumiya, S. Fuke, D. Yang, D. Que, Y. Suzuki and Y. Fukuda, J. Appl. Phys. 90 4219-4223 (2001)
[11] M.S. Chung, W.T. Lin and J.R. Gong, J. Vac. Sci. Technol. B **19** 5 1976-1980 (2001)
[12] K. Shiojima, J. Vac. Sci. Technol. B **18** 1 37-40 (2000)
[13] J.M. Cowley, *Electron Diffraction, An Introduction*, Vol 1, edited by Cowley J M (Oxford University Press, Oxford, 1992)
[14] T. Mori, T. Kozawa, T. Ohwaki, Y. Taga, S. Nagai, S. Yamasaki, S. Asami, N. Shibata and M. Koike, Appl. Phys. Lett. **69** 23 3537-3539 (1996)
[15] R.F. Broom, H.P. Meier and W. Walter, J. Appl. Phys. **60** 5 1832-1833 (1986)
[16] C.A. Pignedoli, R. Di Felice and C.M. Bertoni, Phys. Rev. B. **64** 113301 1-4 (2001)

Figures, Tables and Captions

		N(%)	Ga(%)	C(%)	O (%)	Cl (%)
MBE	reference	64	30	4	<1	<1
	KOH treated	69	27	3	<1	<1
MOCVD	reference	64	28	6	<1	<1
	KOH treated	68	27	3	<1	<1

Table 1: GaN surface atomic weight percentages (atom wt%) of reference and KOH-treated samples determined from a XPS survey spectra. Reduction of the Ga surface content is observed with a corresponding increase of N content as a consequence of KOH treatment, along with a slight reduction of surface C impurities. Traces of O and Cl were also observed.

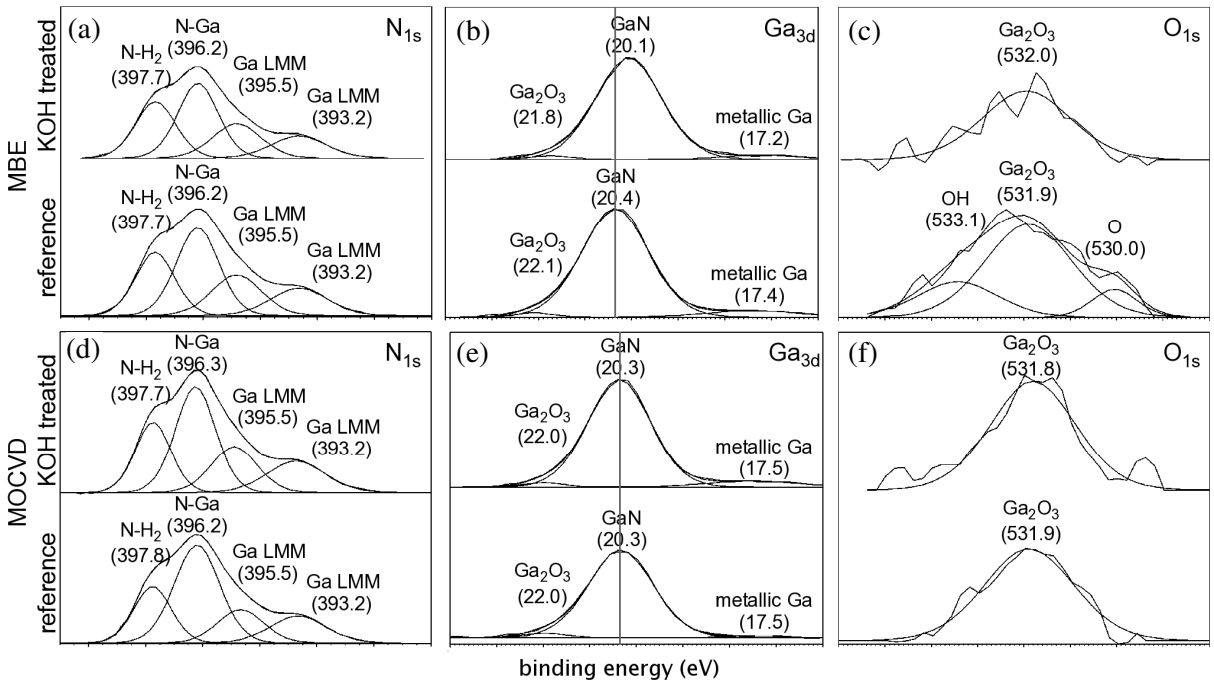

Figure 1: Detailed XPS scans of N1s, Ga3d and O1s peaks showing the shape and energy (eV) of de-convoluted peaks for reference and KOH-treated, MBE- and MOCVD-grown GaN. A significant increase in the N-H_2/N-Ga ratio by ~ 10 % is detected as a consequence of the KOH etching process. For the case of the MBE-grown sample, a -0.3 eV shift in the binding energy of the Ga3d level is observed.

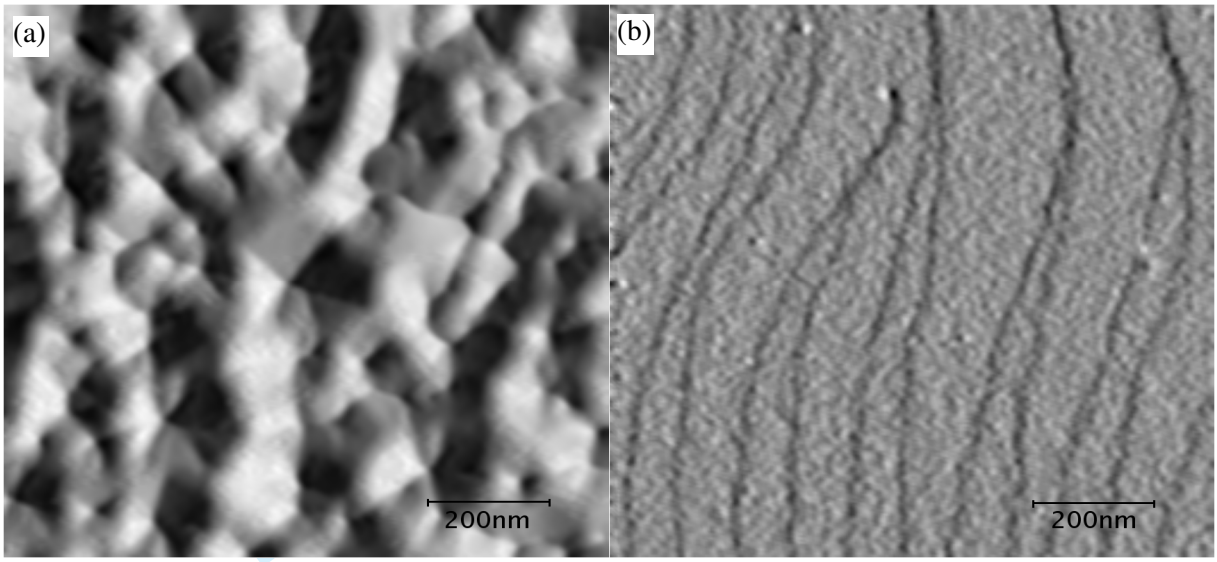

Figure 2: 1 x 1 µm AFM amplitude images of reference HCl-cleaned (a) MBE- and (b) MOCVD-grown GaN/sapphire samples. Corresponding topographical images have heights of 91.07 nm and 4.28 nm, respectively.

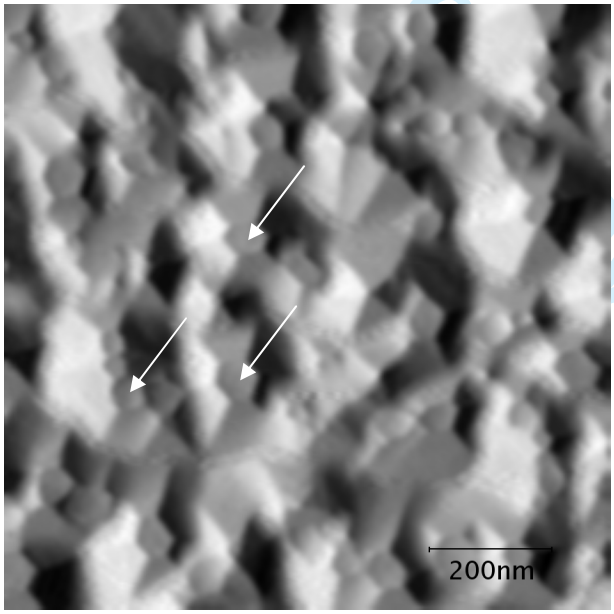

Figure 3: 1 x 1 µm AFM amplitude image of KOH-etched MBE-grown GaN/sapphire, corresponding topographical image has a height of 99.20 nm. The KOH treatment encourages the development of flat-bottomed pits.

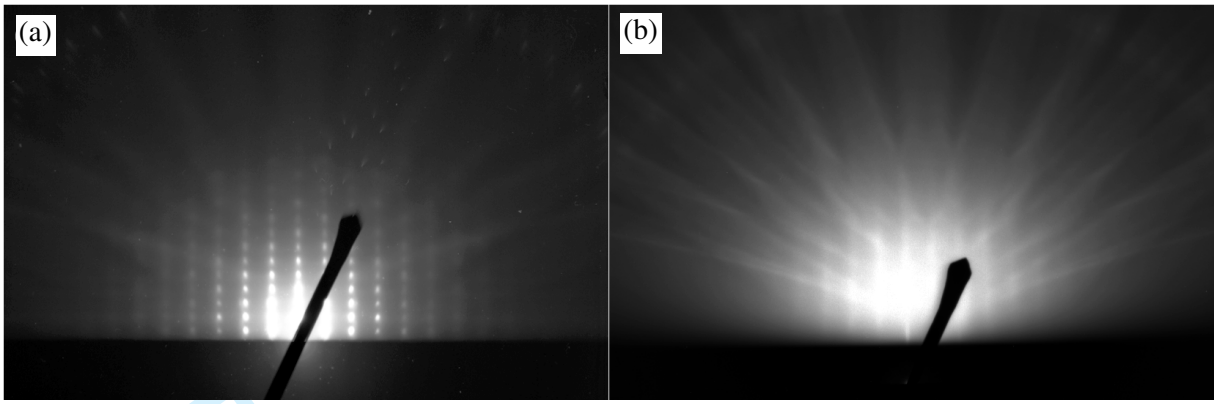

Figure 4: $<\bar{1}120>$ GaN RHEED patterns of reference HCl-cleaned (a) MBE- and (b) MOCVD-grown GaN, indicative of single-crystal hexagonal material with rough and smooth surfaces, respectively.

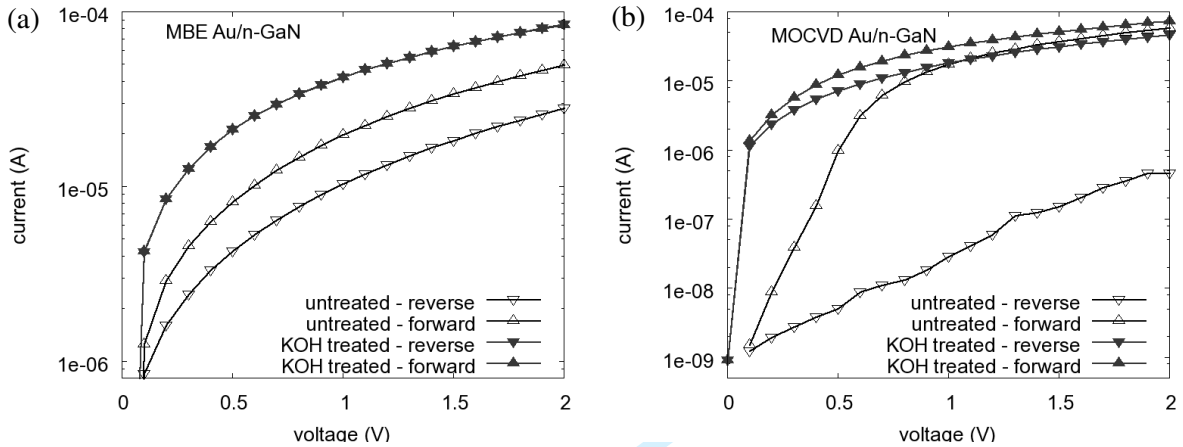

Figure 5: Current-voltage characteristics of Au contacts to reference and KOH-treated (a) MBE- and (b) MOCVD-grown GaN. Au contacts to MOCVD-grown GaN are more strongly rectifying then Au contacts to MBE-grown GaN. The KOH etching treatment results in the formation of more weakly rectifying Au/n-GaN contacts.

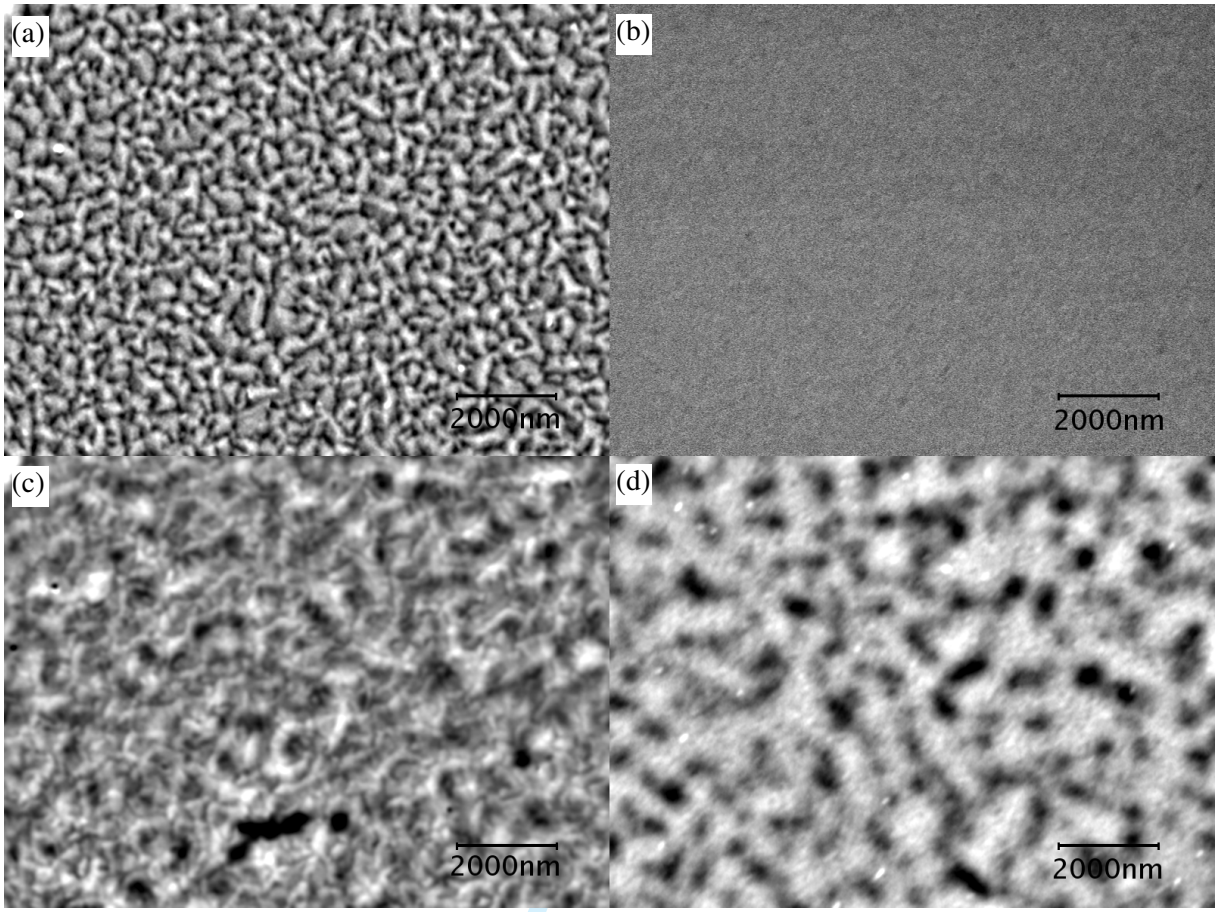

Figure 6: 10 kV correlated SE and EBIC images of Au contacts to reference (a,c) MBE- and (b,d) MOCVD-grown n-GaN. For images recorded in the SE mode, MBE-grown GaN displayed a much rougher surface that MOCVD-grown GaN. For images recorded in the EBIC mode, larger grains were observed for MOCVD- than MBE-grown GaN/sapphire, as expected for these differing growth processes.

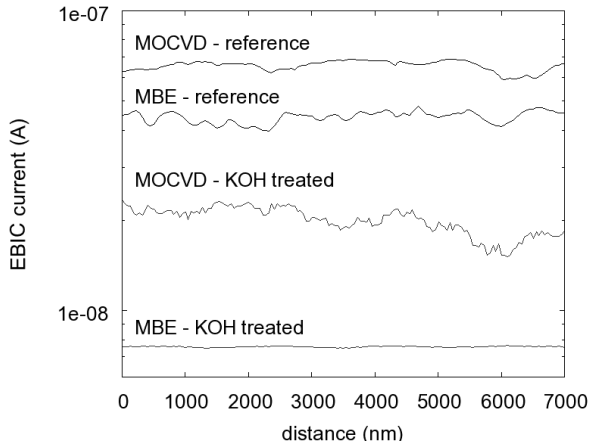

Figure 7: EBIC line scans recorded at an acceleration voltage of 10 kV, under conditions of identical electron beam current and spot size. Peaks in the line profiles correspond to bright areas in the associated EBIC images, considered to be dislocation-free regions, whilst valleys correspond to dark areas within the EBIC images, associated with the sites of dislocations. Averaged values for the EBIC signals and the dislocation contrast are presented in Table 2.

		averaged EBIC signal (nA)		dislocation contrast (%)
		dislocation free site	dislocation site	
MBE	reference	47.0	41.5	12
	KOH treated	7.6	7.5	1
MOCVD	reference	67.0	59.9	11
	KOH treated	18.0	15.9	12

Table 2: Averaged electron-beam-induced currents associated with dislocation and dislocation-free sites and averaged values for the resultant dislocation contrast, comparing reference and KOH-treated, Au-contacted MBE- and MOCVD-grown GaN samples. The reduction in the absolute EBIC current following etching demonstrates that the KOH treatment is associated with an increase in non-radiative recombination activity.

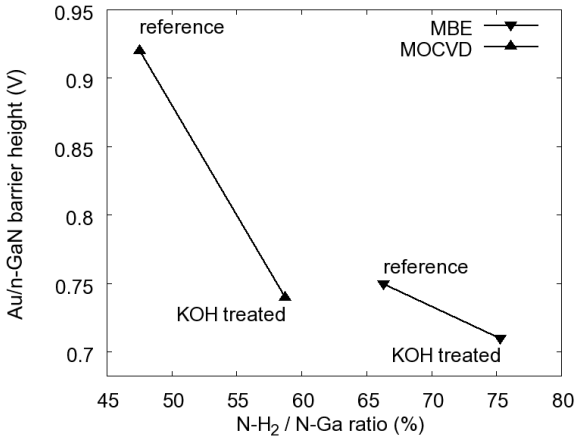

Figure 8: Electron barrier heights of Au/n-GaN extracted from the reverse bias of their current voltage characteristics as a function of the surface N-H_2/N-Ga ratio. A strict linear relationship is not expected as this plot does not take into consideration surface Ga vacancies and C content.